Electric Field and Strain Effects on Surface Roughness Induced Spin Relaxation in Silicon Field-Effect Transistors

Dmitri Osintsev, Oskar Baumgartner, Zlatan Stanojevic, Victor Sverdlov, and Siegfried Selberherr

Institute for Microelectronics, TU Wien, Gußhausstraße 27-29, A-1040 Wien, Austria

Email: {Osintsev|Baumgartner|Stanojevic|Sverdlov|Selberherr}@iue.tuwien.ac.at

Abstract—**The potential of reduction of power consumption and the growth of computational speed achieved by scaling of semiconductor devices is close to exhaustion. Utilizing spin properties of electrons might provide an opportunity for further improvement of the properties of microelectronic-based devices. Since silicon is the main material currently used in microelectronics, we investigate the properties of silicon films and surface layers with respect to their potential applications for spin-based devices. We calculate the electron subband splitting, the surface roughness-induced scattering, and the spin relaxation matrix elements in a silicon-on-insulator spin field-effect transistor for various parameters by applying the perturbative k·p approach and the linear combination of bulk bands method. Shear strain dramatically reduces the spin relaxation matrix elements promising a new opportunity to boost the spin lifetime in a silicon spin field-effect transistor.**

Spin relaxation in silicon, k·p method, spin-orbit interaction, empirical pseudopotentials, shear strain, surface roughness, spin MOSFET

I. INTRODUCTION

Spintronics attracts at present much interest because of opening new concepts for spin-based devices which might be superior to charge based devices. Promising results have been already obtained by utilizing the spin properties of electrons. In order to achieve significant advantages by utilizing spin, materials possessing a long spin life-time and low relaxation rate must be used.

Silicon is composed of nuclei with predominantly zero spin and characterized by weak spin-orbit coupling. Thus, it is a plausible material for spin-based applications. However, the relatively fast spin relaxation observed in electrically gated lateral-channel silicon structures [1] could be an obstacle in realizing spin-driven devices. A deeper understanding of fundamental spin relaxation mechanisms in silicon is urgently needed [2], [3].

In this work we investigate the influence of shear strain and electric field on the subband structure and the spin relaxation matrix elements due to surface roughness scattering. To accurately describe the band structure in silicon in the presence of the intrinsic spin-orbit interaction two different methods are used – the empirical pseudopotential method [4] and the perturbation **k·p** method [2], [4]. Both methods require a small

number of input parameters which are obtained from experimental results. The advantage of the empirical pseudopotential method is that it is applicable for both valence and conduction bands up to electron (hole) energies of a few eVs. However, the **k·p** method requires less computational effort.

First, we generalize the perturbative **k·p** approach [2], [5] to include the spin-orbit interaction. An effective 4x4 Hamiltonian including spin is obtained in the vicinity of the X-point. In contrast to [2], our 4x4 Hamiltonian contains only the two lowest conduction bands for each pair of the valleys. It turns out that within this model the unprimed subbands resulting from the valleys along the k_z axes in an unstrained (001) film, are degenerate without spin-orbit effects included. An accurate inclusion of the spin-orbit interaction results in a large mixing between the spin-up and spin-down states, resulting in spin hot spots along the [100] and [010] axes characterized by strong spin relaxation due to the spin-orbit coupling. These hot spots should be contrasted with the spin hot spots appearing in the bulk system [2], [6]. Their origin lies in the unprimed subband degeneracy in a confined electron system which effectively projects the bulk spin hot spots at the edge of the Brillouin zone to the center of the 2D Brillouin zone.

Shear strain lifts the degeneracy between the unprimed subbands [5]. The energy splitting between the otherwise equivalent subbands removes the origin of the spin hot spots in a confined silicon system, which should substantially improve the spin lifetime in gated silicon systems.

II. THE K·P MODEL

The generalized Hamiltonian including the spin-orbit interaction is written in the vicinity of the high-symmetry point X. The basis is chosen as

$$\begin{bmatrix} (X_1, \uparrow) \\ (X_1, \downarrow) \\ (X_{2\prime}, \uparrow) \\ (X_{2\prime}, \downarrow) \end{bmatrix}, \qquad (1)$$

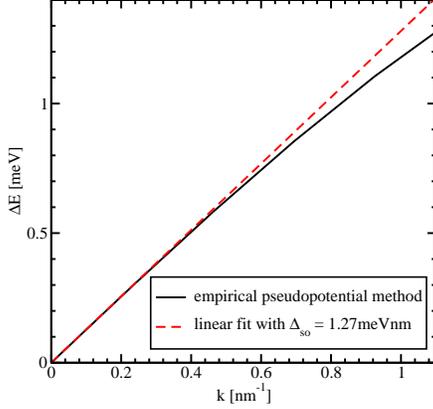where ↑ and ↓ indicate the spin projection at the quantization z – axis.

Figure 1. Empirical pseudopotential calculations of the spin-orbit interaction strength by evaluating the gap opening at the X-point between the X_1 and $X_{2'}$ bands for finite k_x.

The spin-orbit term $\tau_y \otimes (k_x \sigma_x - k_y \sigma_y)$ with

$$\Delta_{so} = 2 \left| \sum \frac{\langle X_1 | p_j | n \rangle \langle n | [\nabla V \times p]_j | X_2' \rangle}{E_n - E_X} \right|, \quad (2)$$

couples the states with the opposite spin projections from the opposite valleys. Here σ_x and σ_y are the spin Pauli matrices and τ_y is the y-Pauli matrix in the valley degree of freedom.

The effective Hamiltonian reads as

$$H = \begin{bmatrix} H_1 & H_3 \\ H_3^\dagger & H_2 \end{bmatrix}, \quad (3)$$

where H_1, H_2, and H_3 are written as

$$H_j = \left[\frac{\hbar^2 k_z^2}{2m_l} + \frac{(-1)^j \hbar^2 k_0 k_z}{m_l} + \frac{\hbar^2 (k_x^2 + k_y^2)}{2m_t} + U(z) \right] I, \quad (4)$$

$$H_3 = \begin{bmatrix} D\varepsilon_{xy} - \frac{\hbar^2 k_x k_y}{M} & (k_y - k_x i)\Delta_{SO} \\ (-k_y - k_x i)\Delta_{SO} & D\varepsilon_{xy} - \frac{\hbar^2 k_x k_y}{M} \end{bmatrix}, \quad (5)$$

Here $j = 1, 2$ numbering the electron bands, I is the identity 2x2 matrix, m_t and m_l are the transversal and the longitudinal silicon effective masses, $k_0 = 0.15 \times 2\pi/a$ is the position of the valley minimum relative to the X point in unstrained silicon, ε_{xy} denotes the shear strain component, $M^{-1} \approx m_t^{-1} - m_0^{-1}$, and $D = 14$eV is the shear strain deformation potential. $U(z)$ is the confinement potential.

III. RESULTS AND DISCUSSION

Since the spin-dependent term in the electron effective Hamiltonian (3) is a linear function of the wave vector k, the proportionality factor (Δ_{SO}) characterizing the strength of the spin-orbit interaction in the conduction band can be found by applying the empirical pseudopotential method. Fig. 1 shows the linear fit with $\Delta_{SO} = 1.27$meVnm to the gap opening at the X-point between the X_1 and $X_{2'}$ bands for finite k_x computed by the empirical pseudopotential method. The value is close to the one reported by Li and Dery [2].
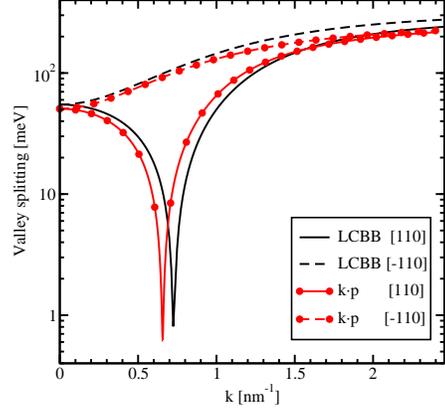

Figure 2. Dependence of the valley splitting on the wave vektor k, for a film of 2nm thickness, the shear strain value is 0.5%.

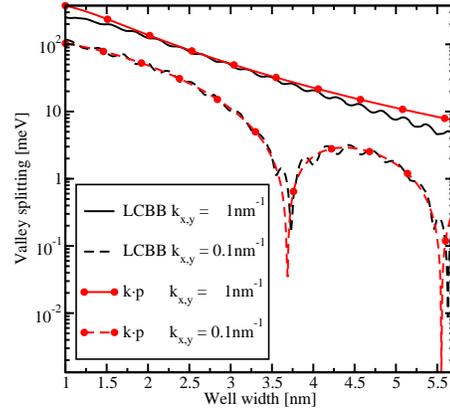
Figure 3. Splitting between the lowest two electron subbands as a function of well width for a shear strain value of 0.5%.

First we investigate the splitting between the equivalent valleys. Fig. 2 shows the splitting between the lowest unprimed electron subbands as a function of the wave vector k taken along [110] and [-110] directions in a confined system. The results computed by the linear combination of bulk bands (LCBB) method [7] and the perturbative **k·p** approach are shown. For the [-110] direction the dependence is smooth without any sharp features. For the curves calculated along [110] direction a sharp decrease of the splitting is observed. Although the positions of the minima calculated by the **k·p** and by the LCBB methods do not match completely, the agreement is quite spectacular.

The valley splitting in a quantum well as a function of the well width is shown in Fig. 3. We chose the in-plane wave vector k along the [110] direction. The results for the wave vectors with the components $k_x = 0.1$nm^{-1}, $k_y = 0.1$nm^{-1} and $k_x = 1$nm^{-1}, $k_y = 1$nm^{-1} are shown for convenience. As predicted [8], [9], the valley splitting develops sharp minima for small values of k. For larger k the valley splitting computed with the **k·p** method decays monotonically when the film thickness is increased. Results obtained by the LCBB method
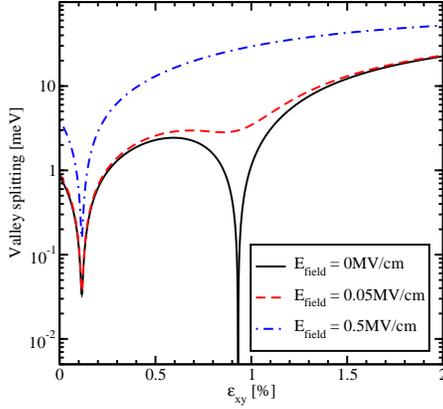
Figure 4. Splitting of the lowest conduction subbands as a function of shear strain for different values of the electric field, the quantum well thickness is 4nm, the conduction band offset is 4eV, $k_x = 0.5$nm^{-1}, $k_y = 0.1$nm^{-1}.

are in good agreement with those obtained by the **k·p** approach. We therefore present below only the results obtained by the **k·p** method.

Now we investigate the effect of shear strain on the valley splitting and spin relaxation due to scattering induced by surface roughness. We assume the spin is injected parallel to the [110] direction throughout the calculations. Fig. 4 shows the dependence of the valley splitting on strain, for the values k_x and k_y being 0.5nm^{-1} and 0.1nm^{-1}, respectively. Without electric field the valley splitting reduces significantly around the strain values 0.116% and 0.931% as shown in Fig.4. With an applied electric field the minimum around the strain value 0.931% becomes smoother, however, for a strain value around 0.116% the sharp reduction of the valley splitting is preserved. For larger field values the valley splitting reduction around the value 0.931% vanishes completely. For the strain value 0.116% the sharp reduction of the valley splitting is still preserved with the bottom value, which is determined by the spin-orbit interaction, only slightly affected by the field. The splitting between subbands depends on $D\varepsilon_{xy} - \hbar^2 k_x k_y/M$ [4] and the degeneracy between the unprimed subbands is lifted, when this term is nonzero. For $k_x = 0.5$nm^{-1}, $k_y = 0.1$nm^{-1} the strain value 0.116% makes the subbands degenerate, in good agreement with the first sharp valley splitting reduction in Fig. 4. The valley splitting is also proportional to $|\sin(kt)|$ [4], [8], [9], where t is the film thickness and k is a function of k_x, k_y, and ε_{xy}. The second minimum in valley splitting around the strain value 0.931% in Fig. 4 is because of the zero value of the $|\sin(kt)|$ term.

The matrix elements of spin relaxation are computed in a standard way to be proportional to a product of the wave functions with the spin up and spin down derivatives [2] at the interfaces. Fig. 5 and Fig. 6 show the spin relaxation matrix elements (normalized to intravalley scattering at zero strain) on the angle between the incident and scattered wave vectors together with the valley splitting for the scattered wave. Oscillations of the valley splitting are observed. In Fig. 5 the sharp increase of the relaxation matrix element is correlated
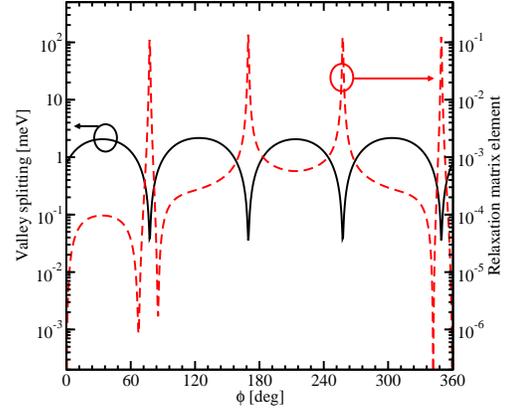

Figure 5. Dependence of the normalized spin relaxation matrix elements and valley splitting on the angle between the incident and scattered waves. The quantum well thickness is 4nm, the conduction band offset is 4eV, $k_x = 0.5$nm^{-1}, $k_y = 0.1$nm^{-1}, $E_{field} = 0$MV/cm, $\varepsilon_{xy} = 0.01\%$.
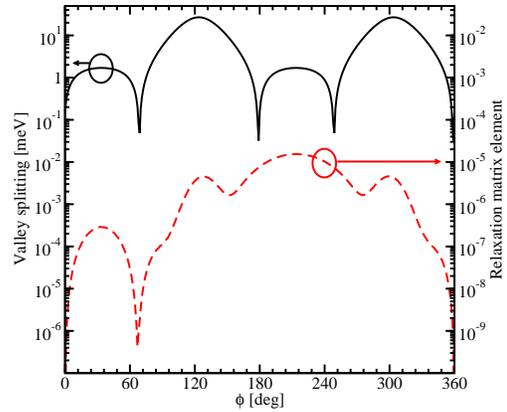

Figure 6. Dependence of the normalized spin relaxation matrix elements and valley splitting on the angle between the incident and scattered waves. The quantum well thickness is 4nm, the conduction band offset is 4eV, $k_x = 0.5$nm^{-1}, $k_y = 0.1$nm^{-1}, $E_{field} = 0$MV/cm, $\varepsilon_{xy} = 0.92\%$.

with the reduction of the valley splitting which occurs for the values of the angle determined by zeroes of the $D\varepsilon_{xy} - \hbar^2 k_x k_y/M$ term. This is the condition of the formation of the so called spin hot spots characterized by the maximum spin mixing. In contrast to Fig. 5, the valley splitting reduction due to the $|\sin(kt)|$ term shown in Fig. 6 does not lead to a sharp increase of the spin relaxation matrix elements.

Fig. 7 and Fig. 8 show the dependences on strain and electric field of the matrix elements for the intra-subband and inter-subband scattering. The intra-subband scattering matrix elements have two decreasing regions shown in Fig. 7. These regions are correlated with the valley splitting minima in Fig. 4. For higher fields the second decreasing region around the shear strain value of 0.931% vanishes. For an electric field of 0.5MV/cm the intra-subband matrix elements are sharply reduced only for the shear strain value of 0.116%. At the same time, the inter-subband matrix elements show a sharp increase around the shear strain value of 0.116%. The electric field does
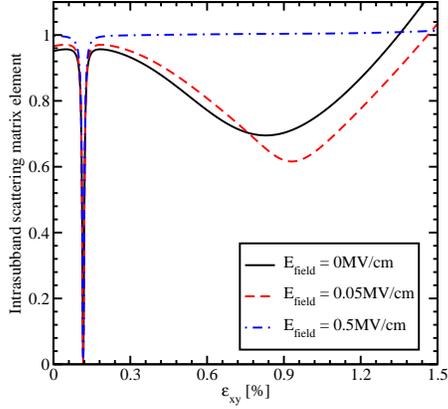
Figure 7. Intravalley scattering matrix elements normalized by their values for zero strain as a function of shear strain for different electric field values.
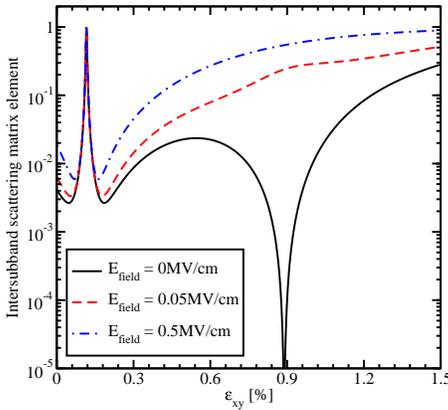

Figure 8. Intervalley scattering matrix elements normalized to the value of the intravalley scattering at zero strain as a function of strain for different electric field values.

not affect much the valley splitting provided by the zero value of the term $D\varepsilon_{xy} - \hbar^2 k_x k_y/M$, and the sharp increase in the inter-subband matrix elements is observed at higher fields as well. At the same time the electric field washes out a narrow minimum around the shear strain value of 0.931% in Fig. 8. With increasing electric field the confinement pushes the carriers closer to the interface, which results in higher inter- and intra-subband scattering matrix elements.

The spin relaxation matrix elements increase until the strain value 0.116%, the point determined by the spin hot spot condition (Fig.9). Applying strain larger than 0.116% suppresses spin relaxation significantly, for all values of the electric field. Contrary to the scattering matrix elements (Fig. 7 and Fig. 8), the relaxation matrix elements exhibit a sharp feature only for the shear strain value of 0.116% at zero electric field. A large electric field leads to an increase of the relaxation matrix elements due to the additional field-induced confinement resulting in higher values of the surface roughness induced spin relaxation matrix elements.
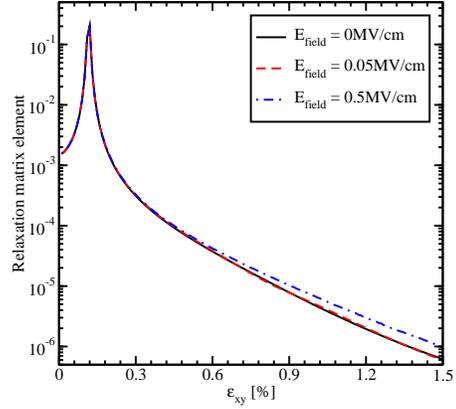

Figure 9. Normalized spin relaxation matrix elements dependence on shear strain for several values of the electric field for $k_x = 0.5nm^{-1}$, $k_y = 0.1nm^{-1}$.

IV. CONCLUSION

We have investigated the lowest unprimed electron subband splitting in a thin film of an SOI-based spin field-effect transistor by the perturbative **k·p** approach and by the linear combination of bulk bands method. We have included the spin-orbit interaction effects into the effective low-energy **k·p** Hamiltonian and have shown a good agreement between the empirical pseudopotential method and the **k·p** approach. Applying the **k·p** method we have demonstrated that the valley splitting minima due to zero values of the $|\sin(kt)|$ term can be removed by an electric field, while the minimum due to $D\varepsilon_{xy} - \hbar^2 k_x k_y/M = 0$ is preserved even for large electric fields. We have shown that, due to the inter-subband splitting increase, the matrix elements for spin relaxation decrease rapidly with shear strain. Thus, shear strain used to enhance electron mobility can also be used to boost spin lifetime.

[1] J. Li, I. Appelbaum, "Modeling spin transport in electrostatically-gated lateral-channel silicon devices: role of interfacial spin relaxation", Physical Review B, 84, 165318, 2011.

[2] P. Li, H. Dery, "Spin-orbit symmetries of conduction electrons in silicon", Physical Review Letters, 107, 107203, 2011.

[3] Y. Song, H. Dery, "Analysis of phonon-induced spin relaxation process in silicon", arXiv:1201:6660v1 [cond-mat.mtrl-sci], 2012.

[4] P. Y. Yu, M. Cordona, "Fundamentals of Semiconductors", 3rd ed., Springer, 2003.

[5] V. Sverdlov, "Strain-induced Effects in Advanced MOSFETs", Springer, 2011.

[6] J. L. Cheng, M. W. Wu, J. Fabian, "Theory of the spin relaxation of conduction electrons in silicon", Physical Review Letter, 104, 016601, 2010.

[7] D. Esseni and P. Palestri, "Linear combination of bulk bands method for investigating the low-dimensional electron gas in nanostructured devices", Physical Review B, 72(16), 165342, 2005.

[8] M. Friesen, S. Chutia, C. Tahan, S. N. Coppersmith, "Valley splitting theory of SiGe/Si/SiGe quantum wells", Physical Review B, 75, 115318, 2007.

[9] A. Valavanis, Z. Ikonic, and R. W. Kelsall, "Intervalley splitting and intersubband transitions in *n*-type Si/SiGe quantum wells: pseudopotential vs. effective mass calculation", Physical Review B, 75, 205332, 2007.